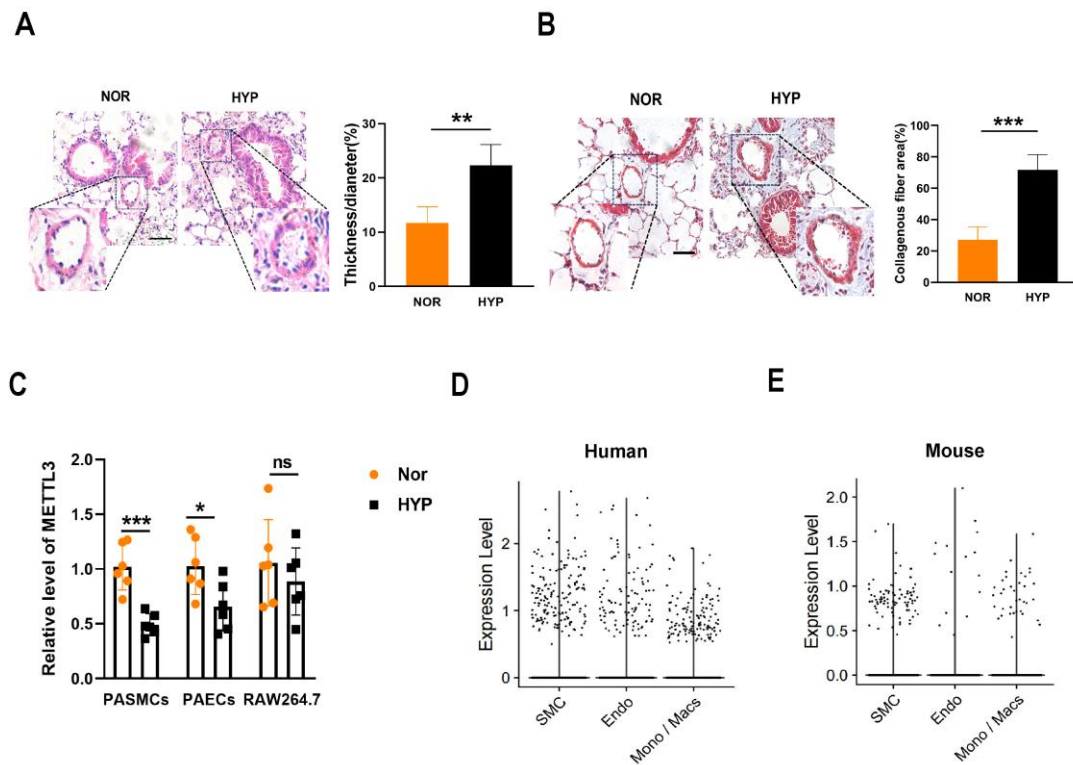# Supplemental Material

Figure S1. The expression of METTL3 in different cells.

A. Pulmonary arterial morphological analysis was performed by using hematoxylin and eosin (HE) staining. Scale bars=50μm (NOR, n=23; HYP, n=22). **B.** Masson staining analysis of the pulmonary vascular remodeling. Scale bars=50μm (NOR, n=23; HYP, n=23) **C.** The expression of METTL3 in PASMCs, PAECs and RAW264.7. (NOR, n=6; HYP, n=6). **D&E.** The analysis on the expression level of METTL3 in various lung cell types, including PASMCs, PAECs, and macrophages in both human and mouse single-cell RNA-seq dataset. Each data point in the figure represents a unique biological replicate. Statistical analysis was performed with one-way ANOVA. The data are presented as the mean ± SD. *p<0.05, **p<0.01, ***p<0.001.

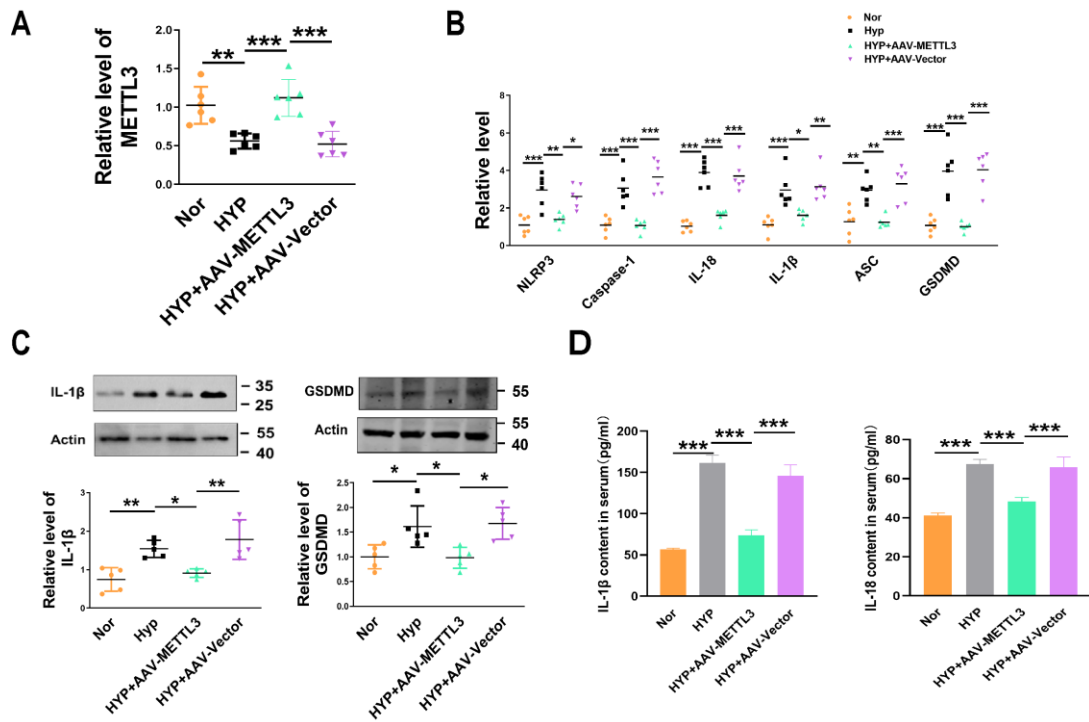**Figure S2. Verification of the effect of METTL3 in mice.**

A The mRNA level of METTL3 overexpression in mice lung tissue was verified using AAV9 viral particles carrying the full-length sequence of METTL3 (Nor, n=6; HYP, n=6; HYP+AAV-METTL3, n=6; HYP+AAV-Vector, n=6). **B.** The mRNA levels of NLRP3, Caspase-1, IL-1β, IL-18, GSDMD and ASC as detected by qRT-PCR (Nor, n=6; HYP, n=6; HYP+AAV-METTL3, n=6; HYP+AAV-Vector, n=6). **C.** The protein levels of IL-1β and GSDMD as detected by Western blot (Nor, n=5; HYP, n=5; HYP+AAV-METTL3, n=5; HYP+AAV-Vector, n=5). **D.** The concentration of IL-18 and IL-1β in each mouse serum as detected by Elisa kit (Nor, n=3; HYP, n=3; HYP+AAV-METTL3, n=3; HYP+AAV-Vector, n=3). Each data point in the figure represents a unique biological replicate. Statistical analysis was performed with one-way ANOVA. The data are presented as the mean ± SD. *p<0.05, **p<0.01, ***p<0.001.
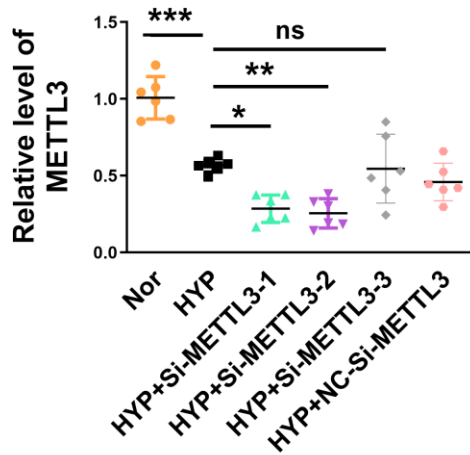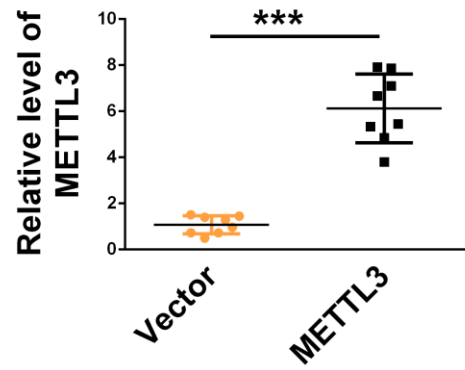
Figure S3. Verification of the efficiency of METTL3 siRNAs and overexpression in PASMCs.

A. Verification of the efficacy of METTL3 in knocking down endogenous METTL3 at the mRNA level in PASMCs (Nor, n=6; HYP, n=6; HYP+Si-METTL3-1, n=6; HYP+Si-METTL3-2, n=6; HYP+Si-METTL3-3, n=6; HYP+NC-Si-METTL3, n=6). **B.** Verification of METTL3 overexpression at the mRNA level in PASMCs transfected with the plasmid vector carrying the METTL3 gene (Vector, n=8; METTL3, n=8). Each data point in the figure represents a unique biological replicate. Statistical analysis was performed with one-way ANOVA. The data are presented as the mean ± SD. **p<0.01, ***p<0.001.
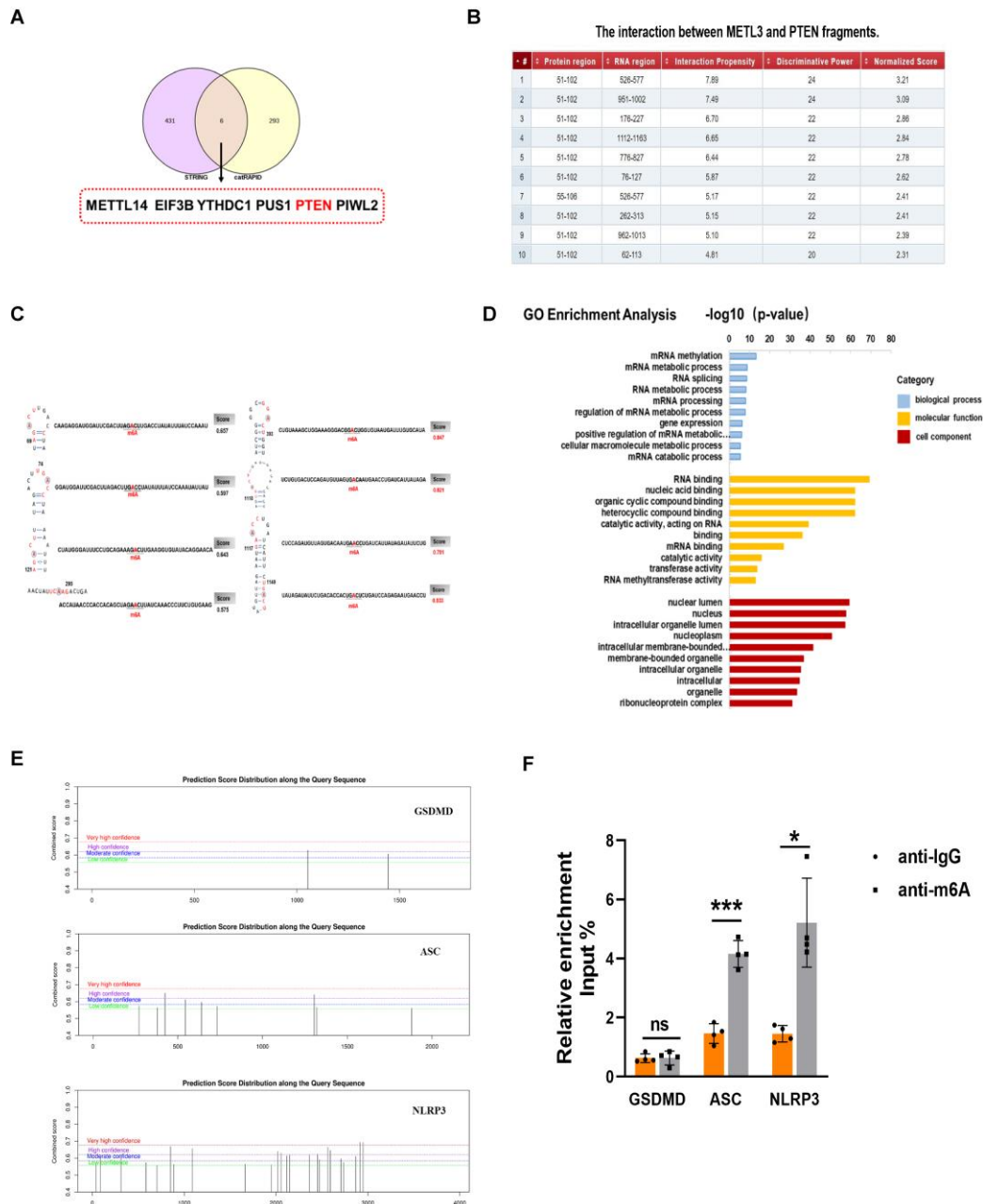
Figure S4. PTEN is a downstream target gene of METTL3.

A. The target mRNAs of METTL3, as predicted by the STRING database and catRAPID database. **B.** Prediction of the binding site of PTEN with METTL3 using catRAPID. **C.** Potential m6A modification sites in the sequence of the PTEN gene. **D.** GO enrichment analysis of METTL3. **E.** Potential sites and regions of m6A modification. **F.** m6A-RIP analysis with an anti-m6A antibody (n=4). Each data point in the figure represents a unique biological replicate. Statistical analysis was performed with one-way ANOVA. The data are presented as the mean $\pm$ SD. *p<0.015, ***p<0.001.
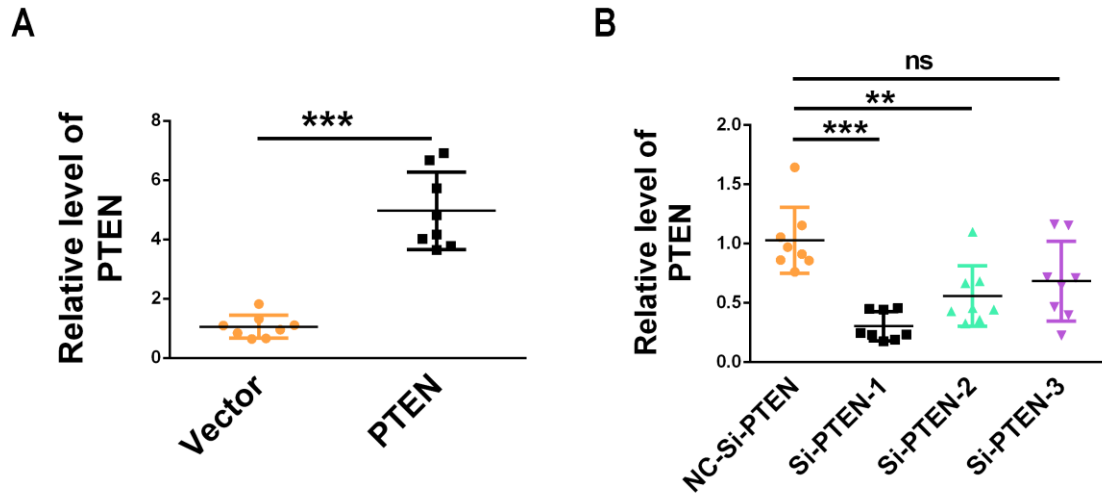
Figure S5. Verification of the efficiency of PTEN in PASMCs.

A. Verification of PTEN overexpression at the mRNA level in PASMCs transfected with the plasmid vector carrying the PTEN gene (Vector, n=8; PTEN, n=8). **B.** The PTEN knockdown efficiency was verified at the mRNA level (NC-Si-PTEN, n=8; Si-PTEN-1, n=8; Si-PTEN-2, n=8; Si-PTEN-3, n=8). Each data point in the figure represents a unique biological replicate. Statistical analysis was performed with one-way ANOVA. The data are presented as the mean ± SD. **p<0.01, ***p<0.001.
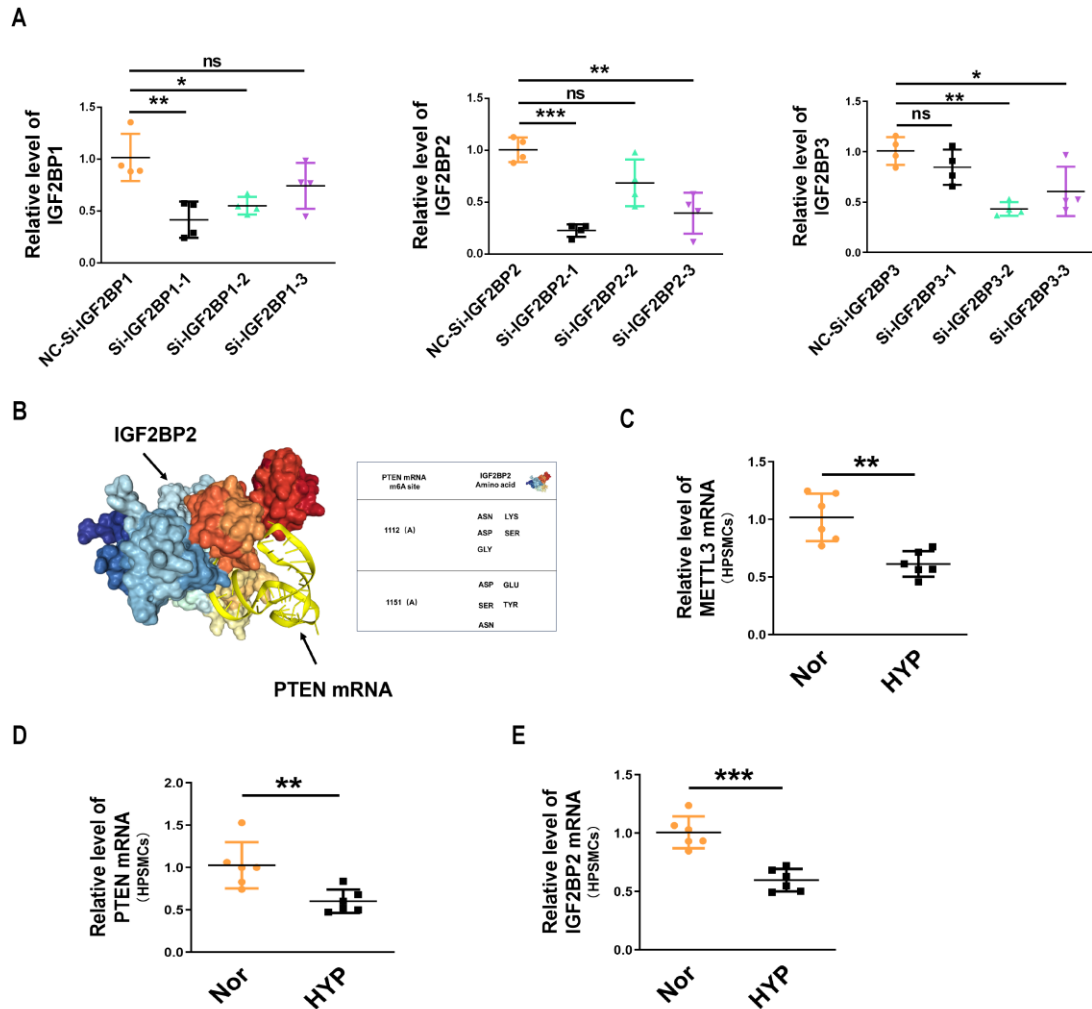
Figure S6. Verification of the efficiency of IGF2BP siRNAs in PASMCs.

A Verification of the efficiency of IGF2BP siRNAs in silencing endogenous IGF2BP2 expression at the mRNA level (NC-Si-IGF2BPs, n=4; Si-IGF2BPs, n=4). **B.** Molecular docking using the online prediction website. **C-E.** The expression of METTL3, PTEN and IGF2BP2 in HPSMCs (Nor, n=6; HYP, n=6). Each data point in the figure represents a unique biological replicate. Statistical analysis was performed with one-way ANOVA. The data are presented as the mean $\pm$ SD. *p <0.05, **p<0.01, ***p<0.001.